

DESIGN OPTIMIZATION AND FINITE ELEMENT ANALYSIS OF A CORKSCREW



By: Mahnoor Azim

The City College of New York
Professor Gary Benenson
ME 37100

Table of Contents

<i>Problem Statement</i>	pg. 03
<i>Pre-Processing for FEA</i>	pg. 04
<i>Failure Testing</i>	pg. 04
<i>Free Body Diagram</i>	pg. 05
<i>Material Selection</i>	pg. 07
<i>Failure Theory</i>	pg. 08
<i>Analytical Model</i>	pg. 08
<i>Solid Modeling</i>	pg. 10
<i>Measurements</i>	pg. 10
<i>Solid Model</i>	pg. 12
<i>SolidWorks Simulation</i>	pg. 19
<i>Boundary Condition Validation</i>	pg. 19
<i>Results</i>	pg. 21
<i>Stress Singularities</i>	pg. 21
<i>Validation of FEM Results</i>	pg. 22
<i>Sensitivity Test</i>	pg. 25
<i>Implications of Design</i>	pg. 31
<i>Conclusions</i>	pg. 32
<i>References</i>	pg. 34

Problem Statement

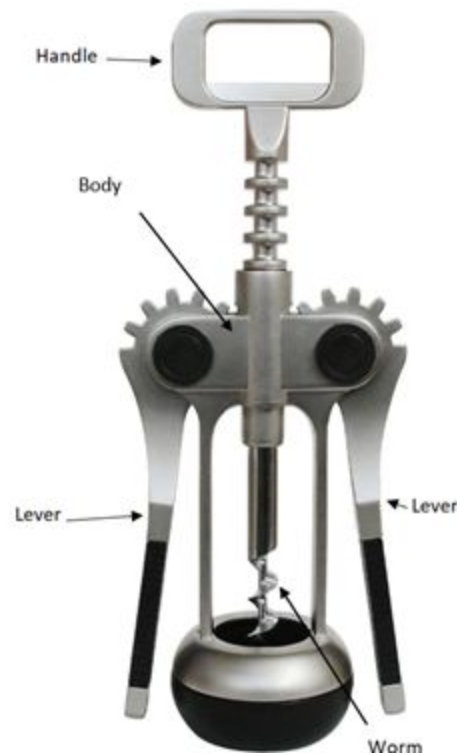


Figure 1: Components of the winged Corkscrew

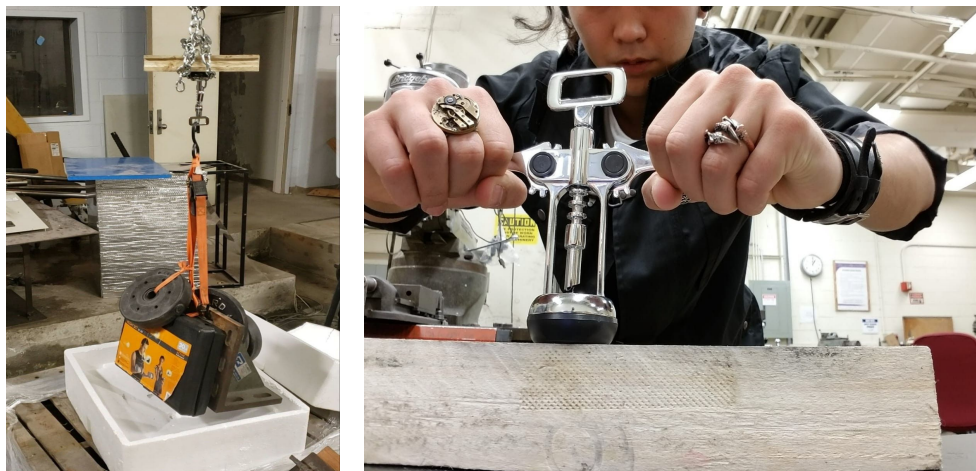
The system that we are trying to analyze is a winged corkscrew. This is a kitchen tool that is typically used in a person's home. The purpose of this tool is to remove corks from bottles. The major components of the system are the handle, the body, the left and right levers, the plastic bearings, and the worm. The specific part of this system that we will be analyzing is the right lever of the corkscrew. The way that this device works is that when the handle is twisted into a cork, the worm is driven into the cork and the levers of the corkscrew are brought up. The levers are connected to the shaft of the handle in a rack and pinion fashion. To remove the cork, a user brings down the levers which in turn pull up the worm along with the cork.

For this project, we are interested in studying the failure of the lever of the corkscrew. We chose this part because corkscrews, or at least the kind that we studied, are inexpensive and widely available. In Professor Benenson's class, we were shown many different examples of failed objects. The one that was most memorable for us was the corkscrew. For the corkscrew example, there were about half a dozen broken corkscrews. We believed this gave us more options than some other objects that we could have chosen. For this corkscrew, we want to understand the conditions that lead to its failure. We want to know how and why this part fails and we hope that FEM can aid us in that endeavor. We also hope that by figuring out why the part fails, we can improve the design of the lever in order to prevent it from failing easily in the future.

Pre-Processing FEA

Failure Testing

At the start of this project, we conducted an experiment to analyze the part of the corkscrew that would fail first. This would be the part that we analyze using FEA. We started the experiment with the prediction that the first part to fail would be the worm. The reason for that prediction was that we had seen multiple winged corkscrews from Professor Benenson's office that had failed at or near this region of interest. Based on that observation, we theorized that the worm was a weak point in the general design of the corkscrew. To test this theory, we conducted an experiment where we fixed the corkscrew by inserting it into a block of wood. Then, we subjected the worm component to tensile force by hanging weights from the handle. We slowly added objects of known weight until we had a sum of 150 lbs hanging from the handle. At this point, we began to worry that the thin handle would fail before the worm, so we chose to halt this experiment. The second part of this experiment was then to leave the corkscrew in the block of wood and to impose the same operating conditions that the corkscrew would be subjected to under normal use. As a reminder, at this point in the experiment, the corkscrew was still inserted into the wood block and because of this the levers were lifted as they would be when a user inserts the worm into a cork. We pulled the levers down as hard as we could to simulate the condition of attempting to remove a stuck cork from a bottle. After applying as much force as we could to the levers a couple of times, we heard a crack. A visual observation confirmed that we had bent the right lever of the corkscrew. The left lever was intact. We believe the reason for this is because the user who applied the force that broke the right lever was right-handed and thus, they were likely able to apply more force with their right hand than they were with their left hand. Another reason for the lack of failure in the left lever is likely because the teeth of the sector gear on the left lever were slipping.



Figures 2-3: First and second part of the experiment.



Figure 4: A comparison between the left hand, non-deformed lever, and the deformed right hand lever.

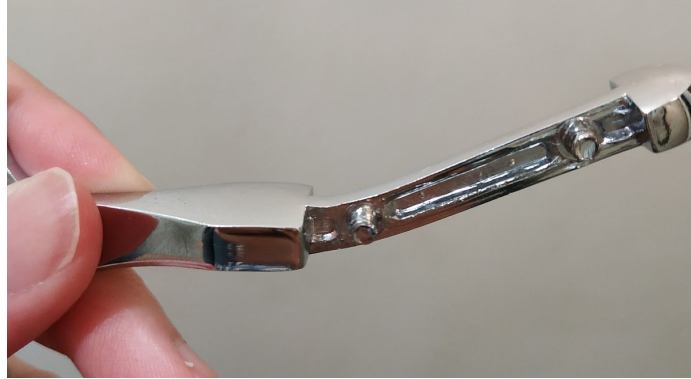


Figure 5: A closeup of the bend in the deformed lever. It was originally completely straight.

Free Body Diagram

Before beginning our FEA studies for the part, it was important to first draw the appropriate free body diagram. We chose to apply a fixed restraint on the faces of one of the gear teeth of the sector gear of the lever. This is to represent the restriction in movement of the lever when it is stuck in the wood. If the lever cannot move, it is because of the contact that exists between the sector gear and the handle of the corkscrew. Next, we chose to model the hole of the lever as having a restraint that would prevent it from translating, but at the same time, allowing it to rotate. In SolidWorks Simulation, this restraint will be applied using a bearing fixture. Finally, the forces that we chose to apply to this model include a downward force at the very end of the lever, and an upward force near the section where there is a change in geometry of the part. These forces are meant to be equivalent, thus creating a bending moment around the area where the lever is thinner. This is to represent the hand of a user operating the corkscrew which is why the forces are around the thinner section of the lever. This is because the thinner section is where the grips are located and where the user is expected to place their hand. The downward force at the far end represents the edge of the users hand as they're pushing down and the upward force represents the part of the user's hand, the thumb, which is under the lever and is pushing up while the hand is pushing the lever down. As for the magnitude of the force, we chose 335N for each force. We chose this value after consulting with multiple people in our lives who frequently workout. We asked them how much they could lift on a lateral pulldown machine. We found that they were able to lift around 125 to 150 lbs. Since we are looking at the “worst case scenario” for

our model, we chose to run simulations imaging that the user can apply 150 lbs of force to the corkscrew. We divided this number in half since only one hand is applying that force instead of two. We then converted that number into Newtons and got a force of approximately 335 N.

After getting the free body diagram for our part, we made predictions about where the maximum stress, maximum displacement, and minimum displacement would be. We predicted the maximum stress would occur at the location where the red mark is labeled in Figure 7. This is because there is a change in geometry at this location of the lever, and the moment that is present in this case, would likely produce high concentrated stress there. We made our prediction for the maximum displacement in green, and the minimum displacement where the diagram is marked in blue. Since the end of the lever is free and being subjected to the loading, it would probably have the greatest displacement. Since the gear tooth is the furthest away from the loading and also fixed, it would have the minimum displacement.

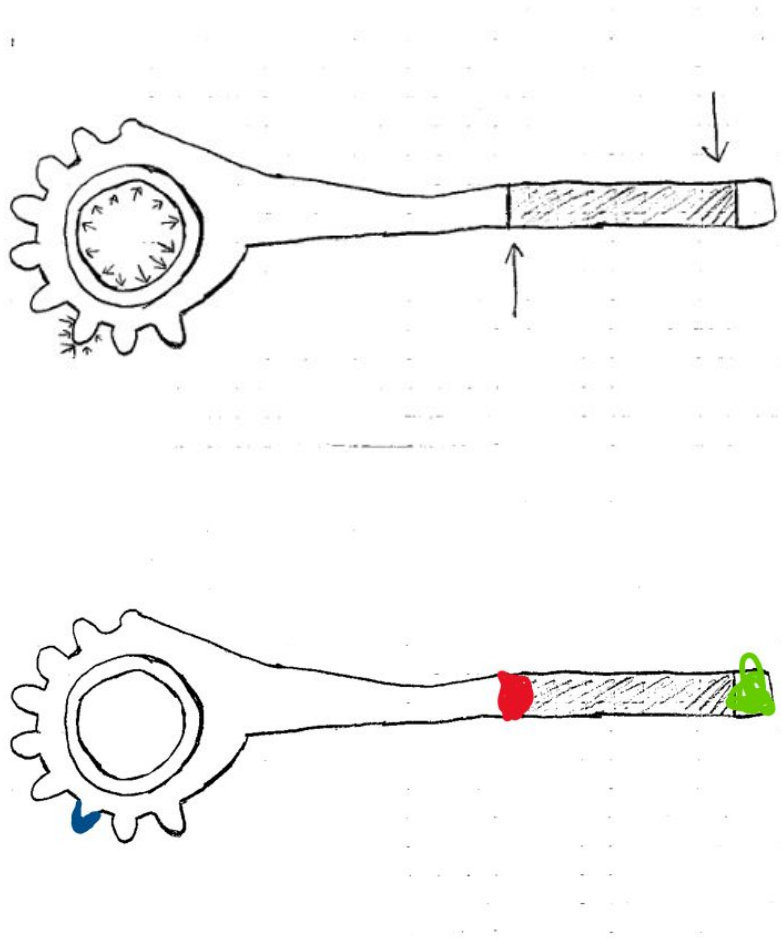
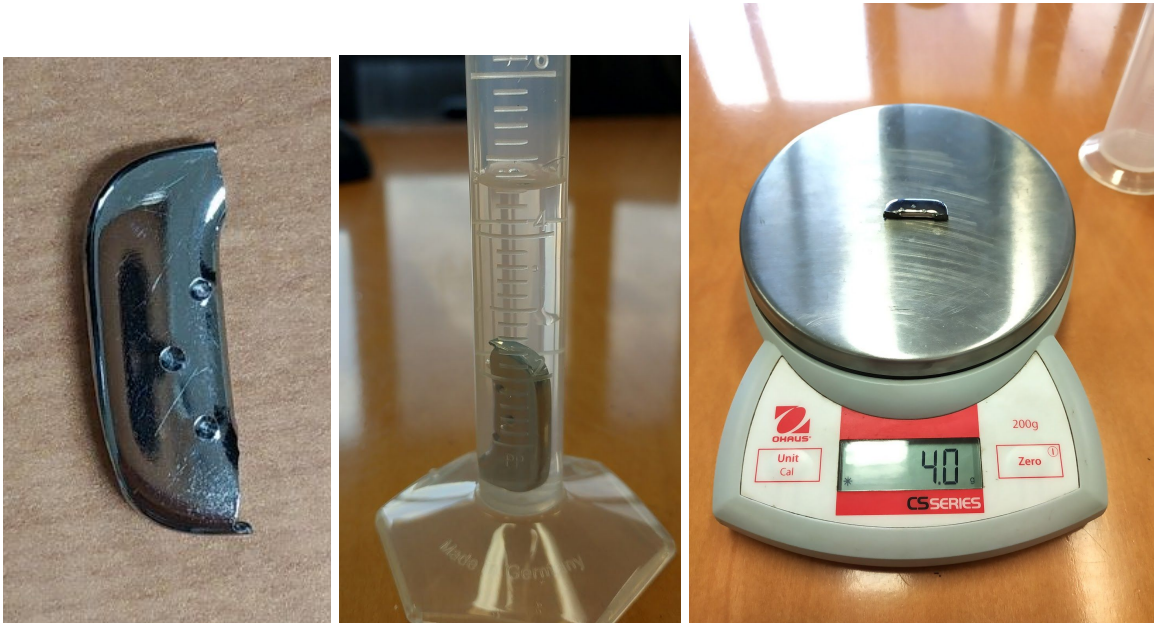


Figure 6: Free body diagram of the lever under the boundary conditions we chose to apply.

Figure 7: Same free body diagram of lever labeled with predictions: red for maximum stress, green for maximum displacement, and blue for minimum displacement.

Material Selection

After we had discovered which part of the corkscrew failed first for our scenario and modeled it, we were still not ready to conduct FEA because we first needed to determine what material the part was made of. This revealed itself to be very challenging. We started with little idea of what the part was made of but we were able to narrow it down quite a bit starting with a suggestion from Professor Benenson that the material was stainless steel. First, we conducted a Rockwell Hardness test by cutting a piece off of the handle of the corkscrew, which we predicted was the same material as the lever. From this, we concluded that the part had an HRC reading of 40. We also found the approximate density of the metal by finding the mass and volumetric displacement using a scale and a graduated cylinder. From these tests, we found a density of 5.71 g/cc with a systematic uncertainty of 0.29 g/cc. By holding a magnet to the part, we were also able to determine that it was non-magnetic. From the hardness, we were able to find an approximate ultimate tensile strength for the material [1]. The ultimate tensile strength should be approximately 1296.21 MPa. This information will help us in narrowing down what material we're using. Now, based on all of this information and with the aid of matweb, we found what we believe is likely to be our material. This material is AK Steel 301 Austenitic Stainless Steel that is cold-worked and full hard. Some of our reasons for believing this is because the hardness of this steel is HRC 41. This steel is austenitic and as a result is nonmagnetic. The ultimate tensile strength of this steel was close to the ultimate tensile strength found for our material by the use of the hardness reading. The ultimate tensile strength for this kind of steel is 1276 MPa. Assuming this is our material, the yield strength is approximately 965 MPa.



Figures 8-10: Hardness test of a piece of the corkscrew, volumetric displacement test, and mass calculation.

Failure Theory

After concluding that our material was stainless steel, we knew that we were looking at ductile failure. Since the deformed lever from our experiment had bent with no sign of fracture, this confirmed again that there was ductile failure involved in the deformation of the handle. In order to analyze this type of failure, the proper failure theory needed to be applied. For our case, we chose to use the von-Mises failure theory of ductile materials, which states that yielding occurs in a part when the maximum von-Mises stress surpasses the yield strength of that material. In our case, once the maximum von-Mises stress exceeded the yield strength, the part had plastically deformed. This theory is explained by a stress and strain graph of a ductile material like ours. This is shown in figure 11. The von-Mises failure theory of ductile materials will be used in our FEA studies in order to help indicate which areas of the part are within the plastic or elastic range.

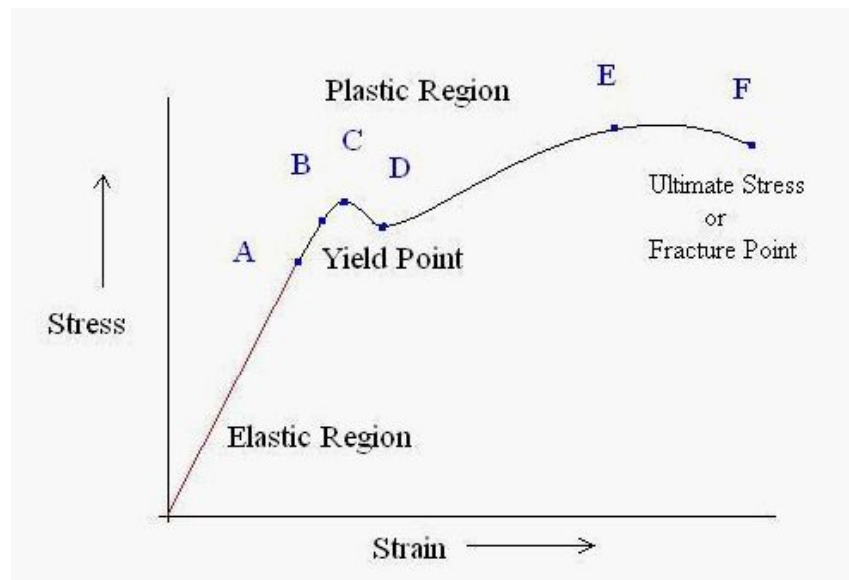


Figure 11: Stress-Strain graph for ductile materials.

Analytical Model

Using knowledge from our ME 330 course, we can represent the lever under the loading conditions applied by treating it as a cantilever beam. The lever can be thought of as a cantilever beam with a fixed end at one end and an applied loading from the top at the other end, as seen in the figure shown below. Using this analogy, we expect the lever to be in tension at the top, and in compression at the bottom with a higher stress concentration near the fixed end. Our part had

failed around this area of the lever where the geometry had changed. Based on the prior project of FEM 1 done in this class, we already know that a high stress concentration is present where there is a sharp change in geometry. If the FEA studies show that there is indeed a higher stress concentration near this area, an application of fillets at the sharp corners of the lever will be implemented to help relieve this stress. Using a variation of fillet radius sizes on the corners, we will perform a sensitivity test for the fillets.

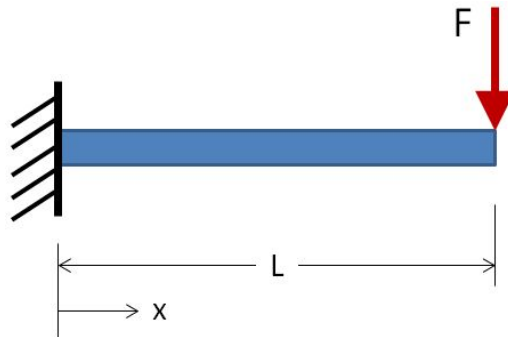


Figure 12: Diagram of a cantilever beam under loading with a fixed end.

Analytical Solution

$$\begin{aligned}
 L &= .092m, F = 335N, b = .003m, h = .0066m, c = \frac{h}{2} = .0033m \\
 M &= F(L) = 335N(.092m) = 30.82 N * m \\
 I &= \frac{1}{12}bh^3 = \frac{1}{12} * .003 * .0066^4 = 718.7nm^4 \\
 \sigma &= \frac{Mc}{I} = \frac{30.82 N * m * .0033m}{718.7nm^4} = 1,415.13 MPa
 \end{aligned}$$

Solid Modeling

Measurements

For the measurements of the lever we used a digital calliper shown in Figure 13. The measurements included the overall length, the thickness of the part, and diameters and radii of the circular geometries.



Figure 13

For better visualization of the dimensioning process, we traced the outline of the lever on a piece of paper along its top view which you can see in Figure 14.

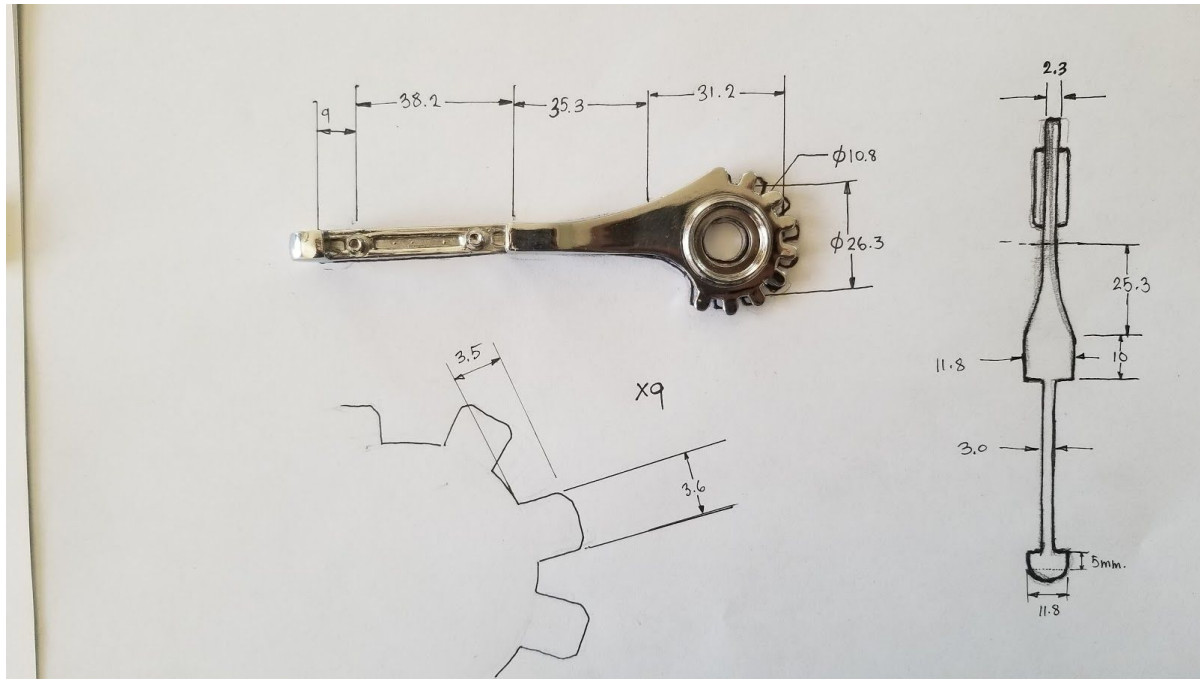


Figure 14

Eventually, the lever was split up in four subparts that would be modeled systematically from head-to-leg manner. The schematics can be seen in Figure 15 below. This provides ease in both taking dimensions and performing future solid modeling procedures.

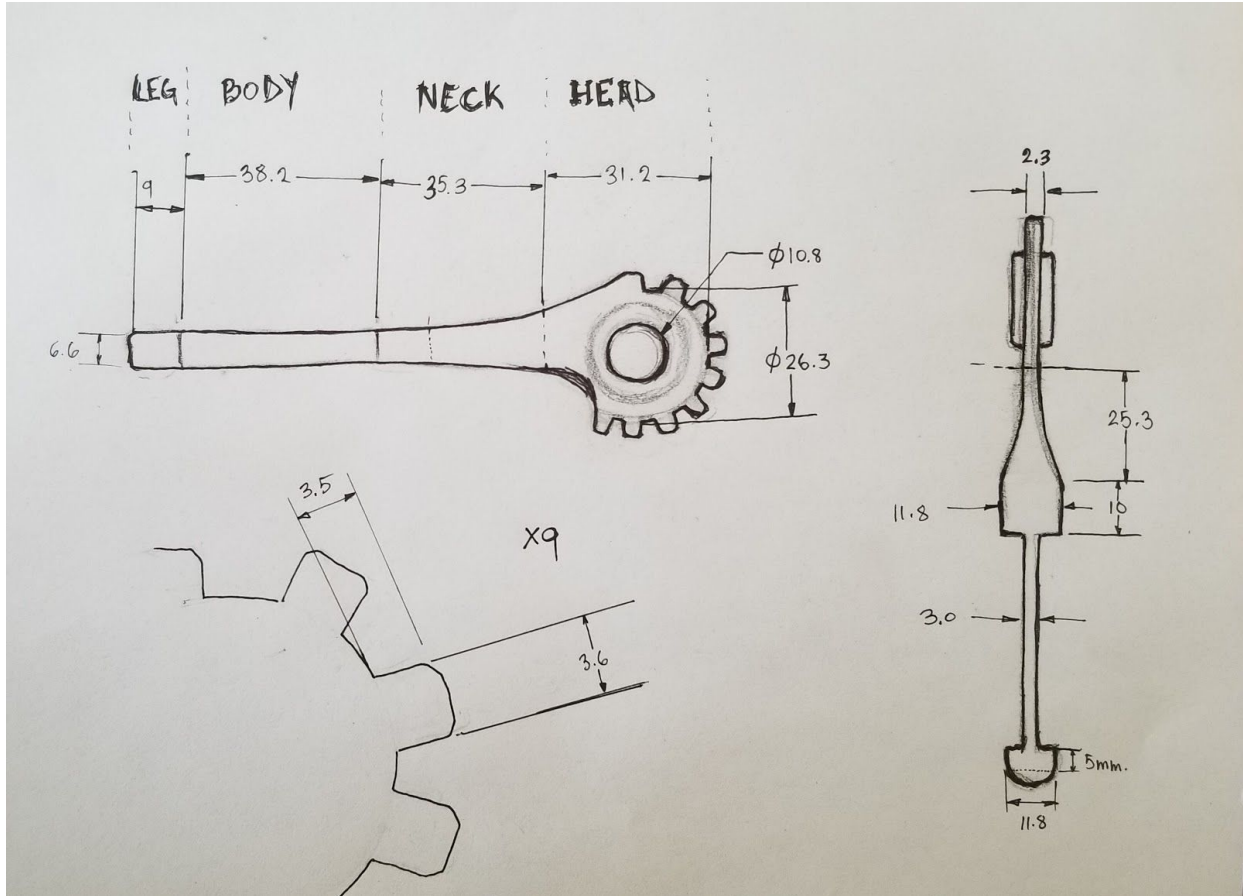


Figure 15

Solid Model

Step 1

On the front plane, two circles were sketched inside of one another with diameters of 10.8mm and 26.3mm, which would represent the cutout and the diameter of the geared head without teeth respectively. On the surface of the outer circle then, the geometric shape of the single tooth of the gear was sketched, as shown in Figure 16. Using the Circular Sketch pattern feature, 8 more teeth were added along the outer curve. This process is shown in Figure 17.

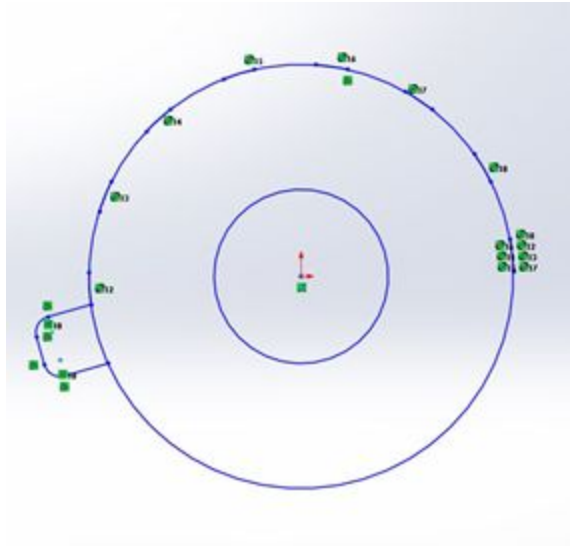


Figure 16

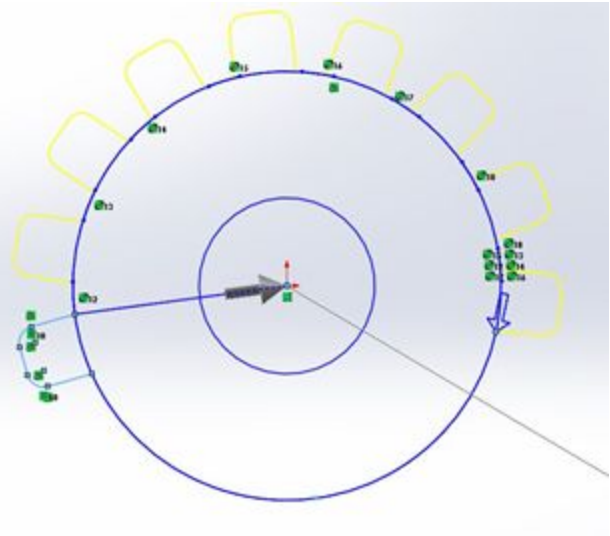


Figure 17

After the appropriate dimensions were set and the outline of the head was sketched, it was extruded to the thickness of 2.3mm. This can be seen in Figures 18 and 19.

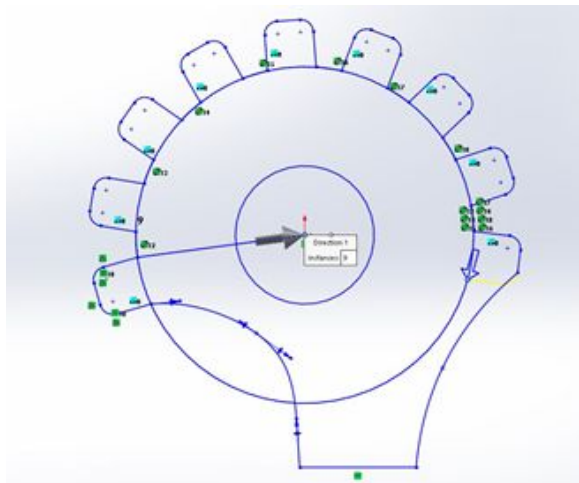


Figure 18

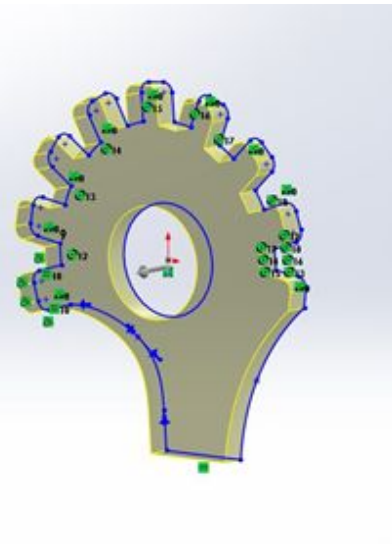
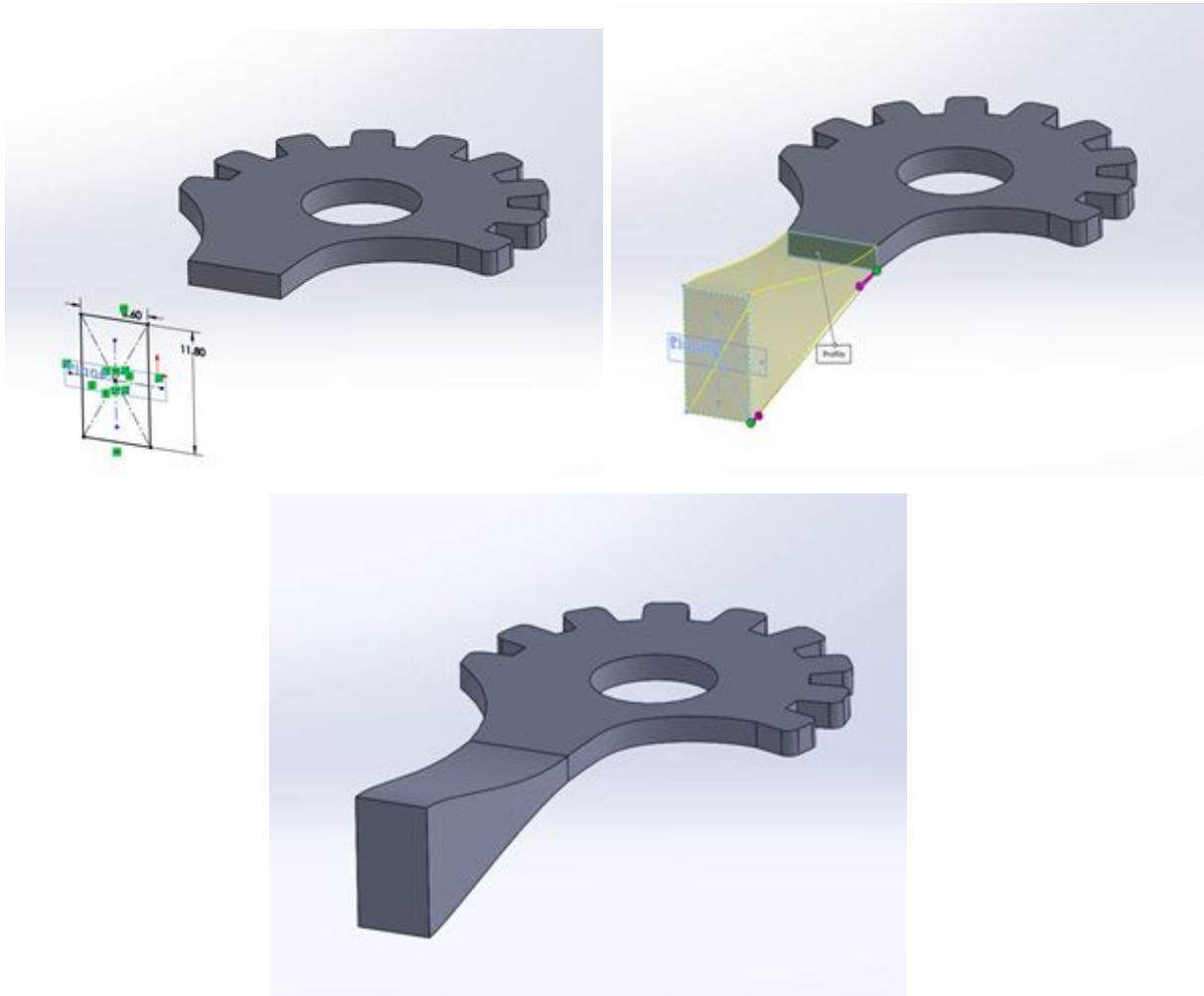


Figure 19

Step 2

After the Head part was completed, the parallel to its bottom face plane was created, at a distance of 25.3mm. So the region in between with a new plane and bottom face, would be where

part of Neck would go that has non-homogeneous cross sectional area. The sketch of a rectangular cross section was drawn on the plane (6.6 X 11.8mm) and then two rectangles were lofted creating a solid piece. It is necessary to mention that the normal vectors were set up and used during the Loft process. This is called setting up Start/End Constraints and both of them were set to Normal to Profile in order to avoid discontinuous profiling between which in this case, were the Head and Neck parts. These procedures are visualized in Figures 20-22.



Figures 20-22

Step 3

By still keeping the same orientation in mind of where the bottom face is, we can now extrude the remaining part of the Neck region to the length of 10mm. This is shown in Figure 23 below.

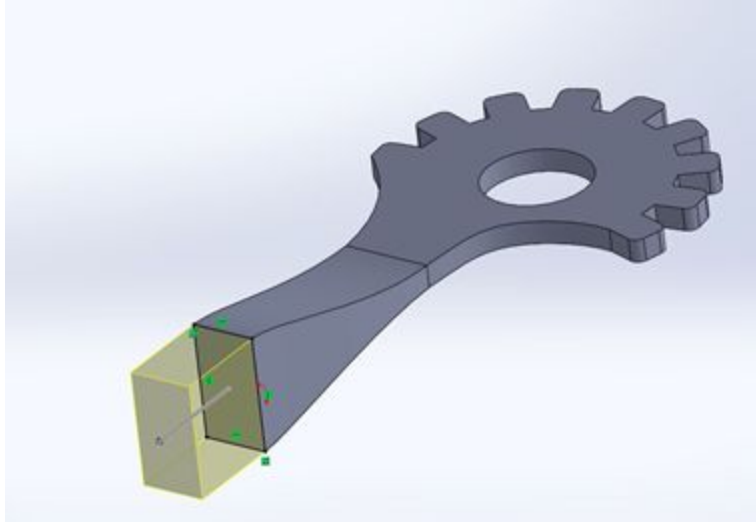


Figure 23

Step 4

In this step we are going to create a Body part of the lever. We sketch the rectangular cross-section of the shaft on the bottom face of the Neck which is where we left off in Step 3. The sketch was then extruded so that the shaft would have a distance of 38.2 mm. (Figures 24 and 25)

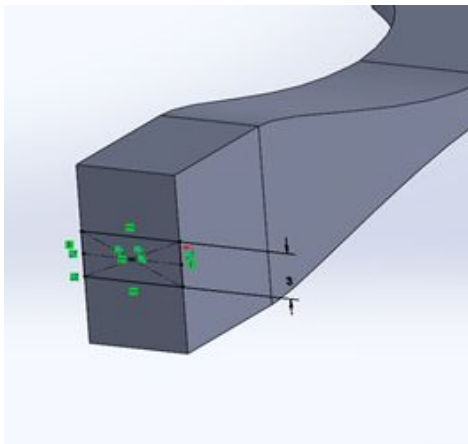


Figure 24

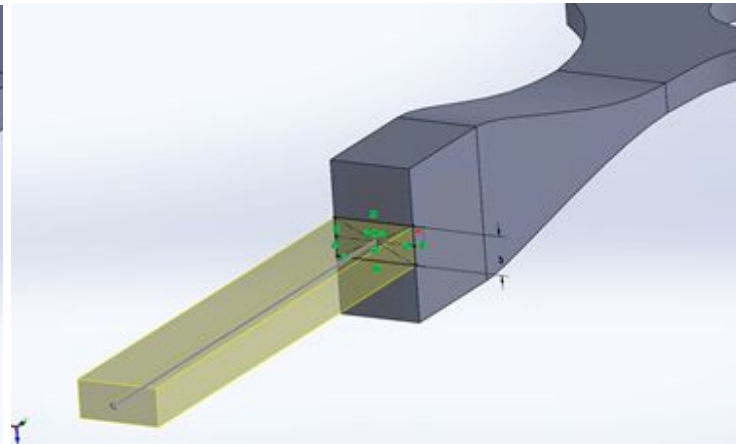


Figure 25

Step 5

Now we can get to the Leg part. The initial procedure is similar to the previous 2 steps, in that we just need to create a new cross-section with dimensions of 6.6 X 11.8mm, and extrude the sketch to a length of 5 mm. (Figures 26 and 27)

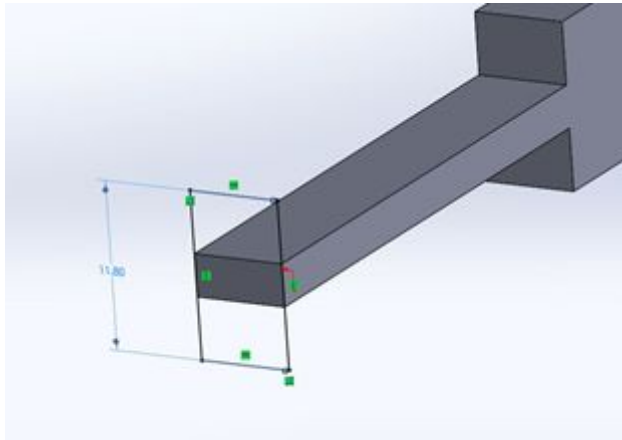


Figure 26

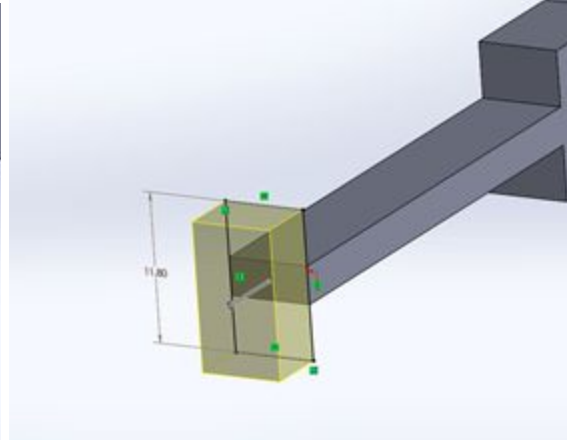


Figure 27

Step 6

In this step we first set a plane that cuts vertically through the middle of the cross section, which can be seen in Figure 28. On this plane, the semi-circular outline was created, however in the middle it was split up in order to make two equivalent circular paths from both sides, which can be seen in Figures 29-30.

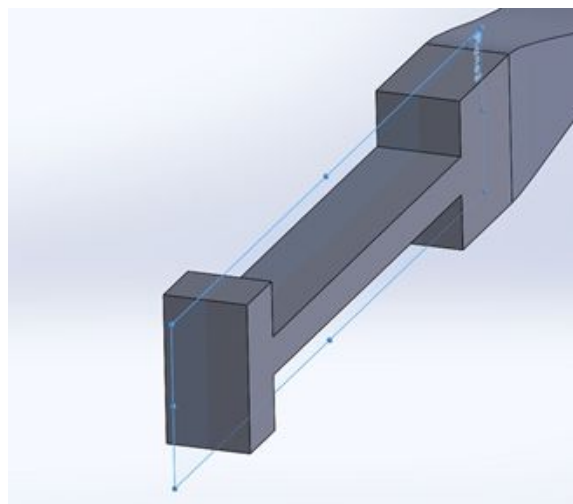
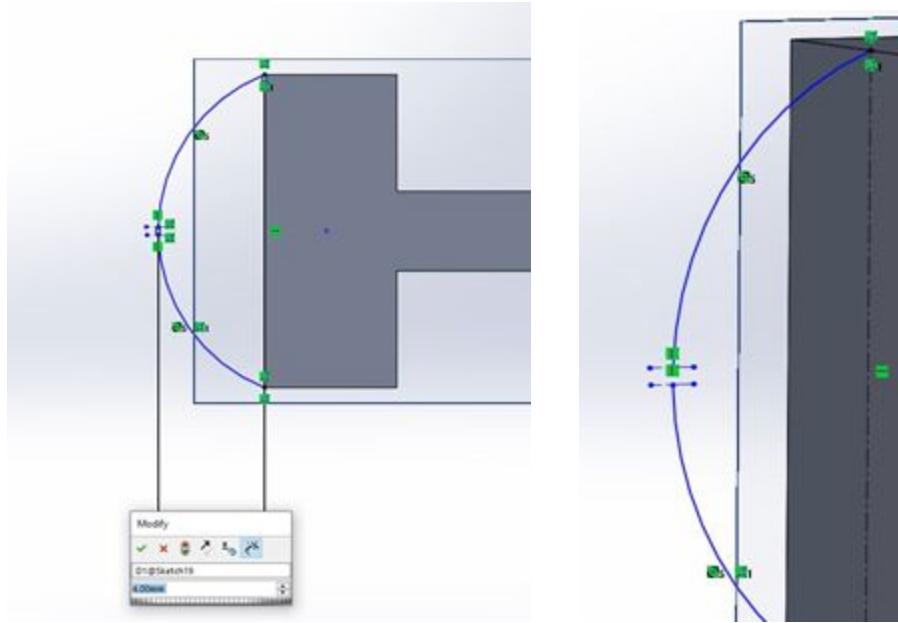
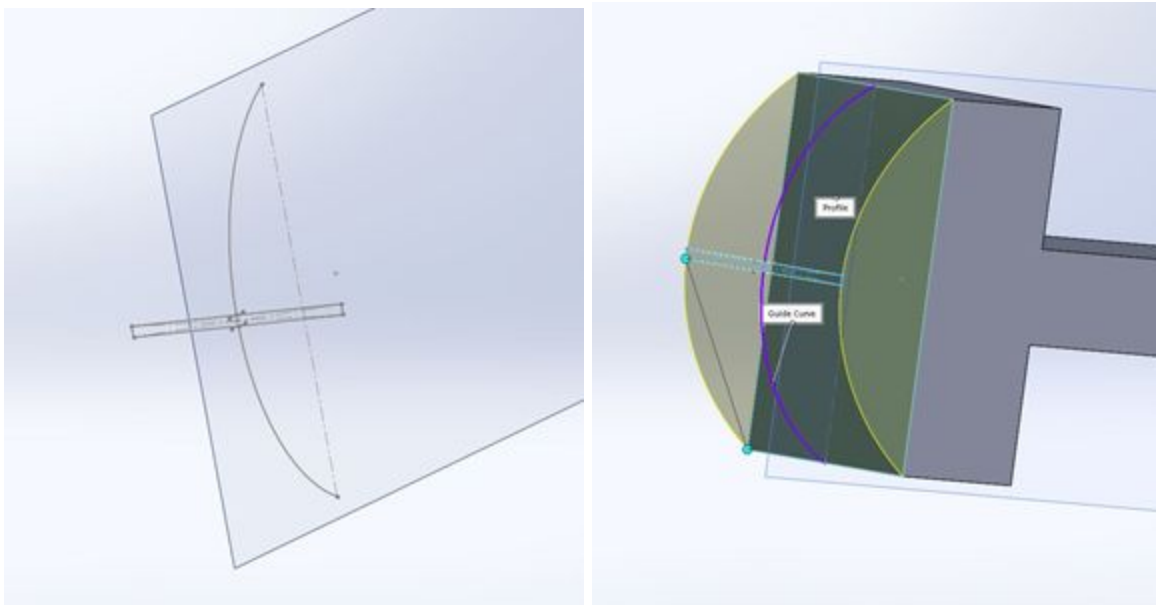


Figure 28



Figures 29-30

Perpendicular to these two new curves and parallel to the bottom face, we then sketch a rectangle that would serve as the final sketch for the Loft procedure. Meanwhile, the two semi-circular lines would serve as the Guide Curves between the bottom face of the solid part and the newly created rectangular sketch. This process is visualized in Figures 31 and 32 below.



Figures 31-32

The final result of the Solid Model is depicted in Figure 33 below.

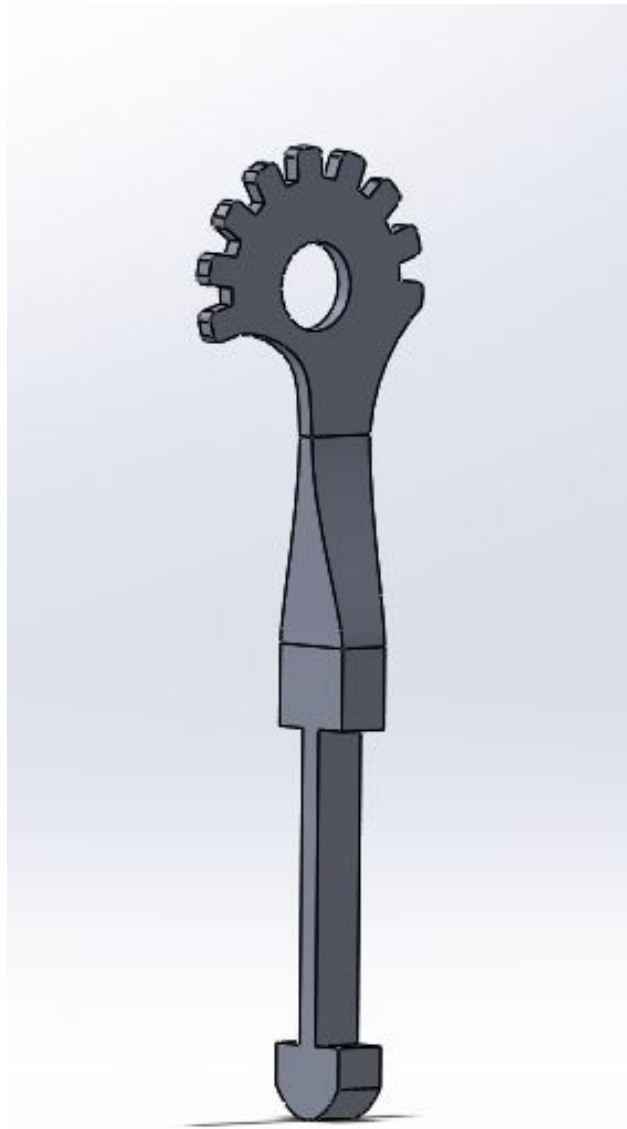
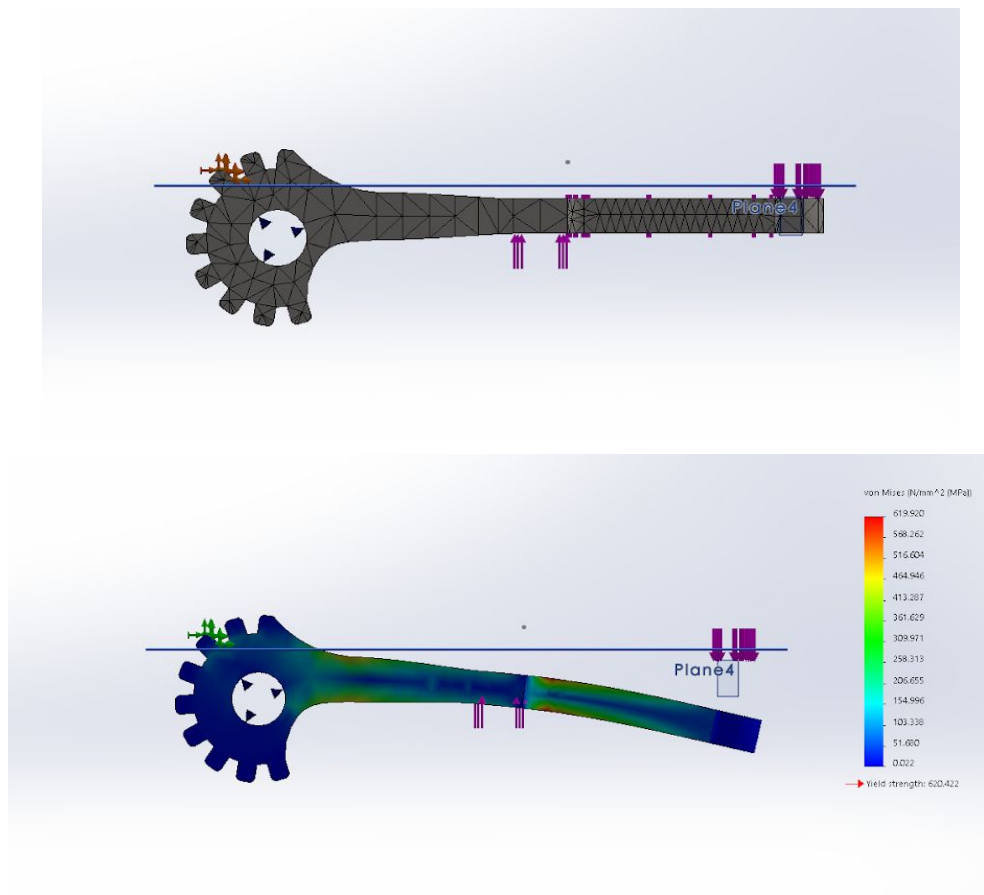


Figure 33

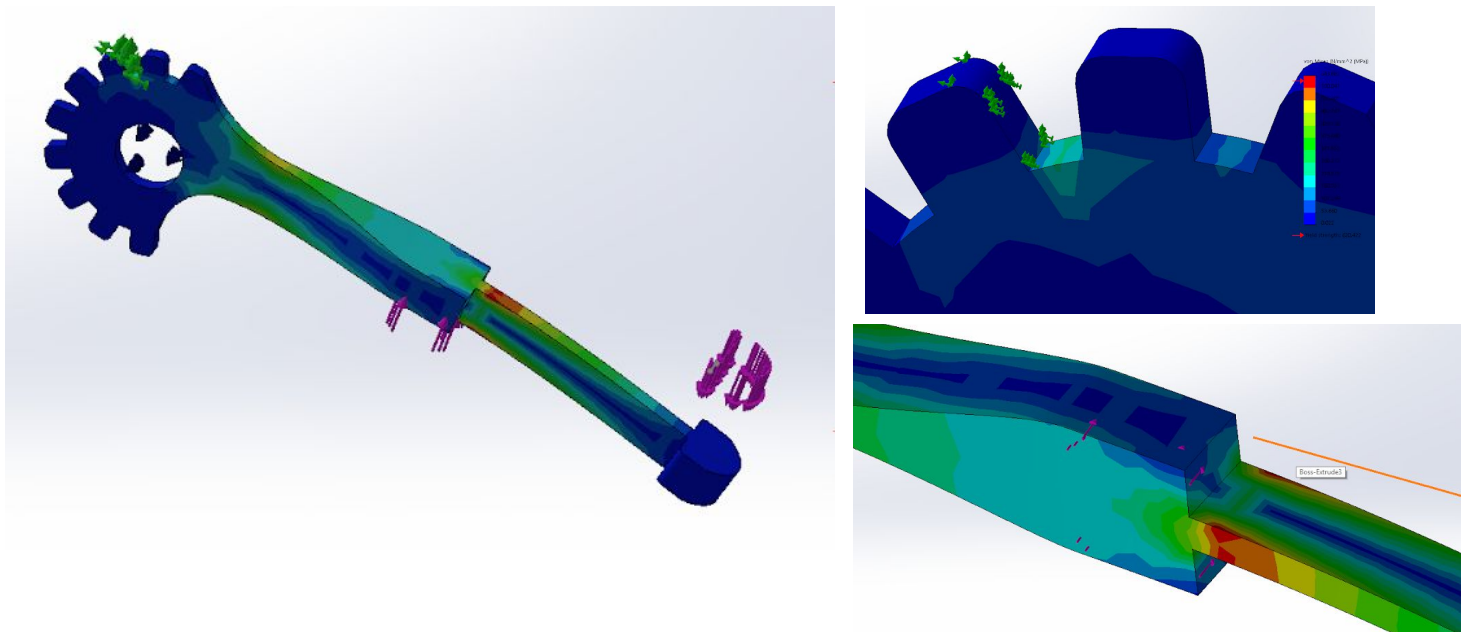
SolidWorks Simulation

Boundary Conditions Validation

Based on our free body diagrams shown in Figure 6, we applied the proper boundary conditions for the experiment that we performed. Four boundary conditions were implemented: a fixed geometry around one of the teeth of the sector gear, a bearing in the hole of the sector gear which allows rotation of the lever, and the two forces that represent a person's hand. One force was applied pointing down at the end of the lever and the other was applied pointing up near the location of change in geometry. Both of these forces had a numerical value of 335N which was calculated as a worst case scenario force of 125 to 150 pounds. We validated these boundary conditions by comparing the resulting stress and displacement plots to our predictions of where the locations of maximum stress, and maximum and minimum displacements would be. The results were not that far off as the maximum displacement was indeed at the far end of the lever, the maximum stress was near the location of change in geometry, and the minimum displacement was at the sector gear teeth. The meshing and simulation as shown in Figures 34-39.



Figures 34-35: Meshing of the SolidWorks model and the resulting stress plot.



Figures 36-38: Resulting stress plots for the implemented boundary conditions on the part.

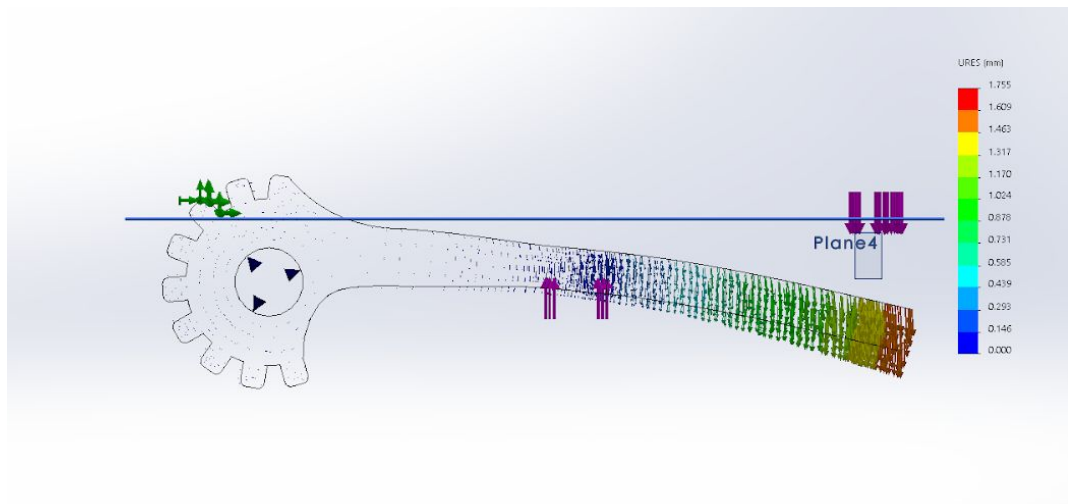
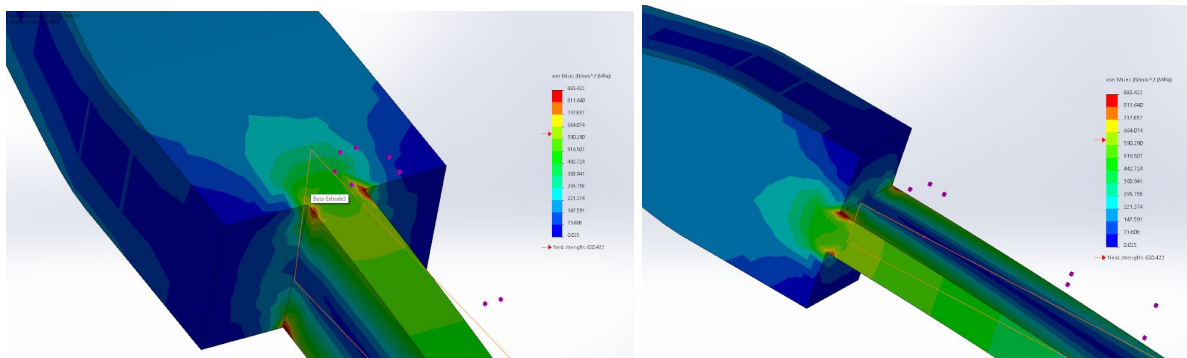


Figure 39: Resulting vector plot for the displacement of the model under loading.

Results

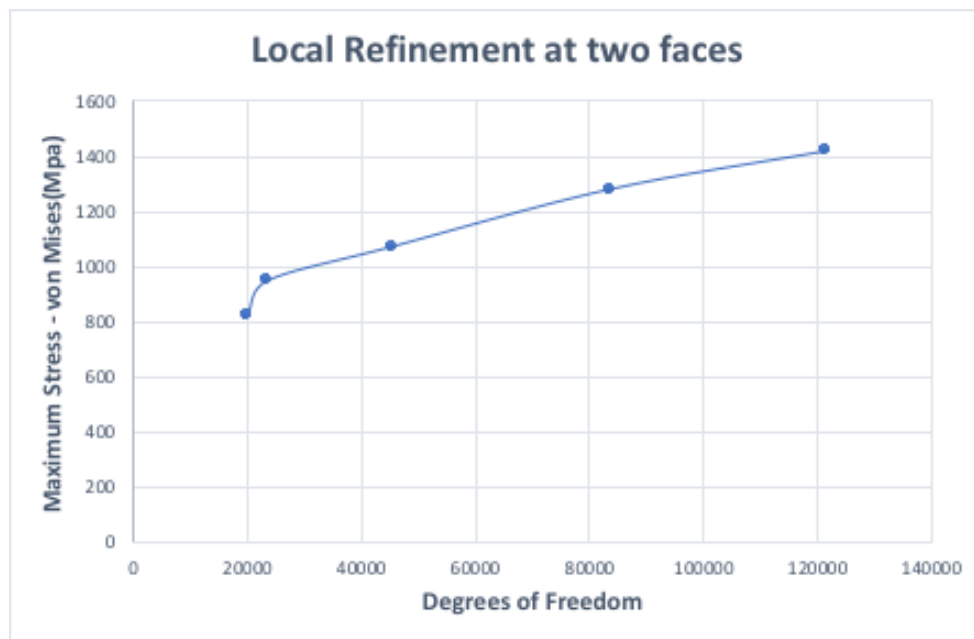
Stress Singularities

After we had found the right boundary conditions for our model, we decided to perform a convergence study. After running some simulations on our model, we noticed that the data never converged. We came to the conclusion that the current model would never converge since there were some stress singularities on our model as seen in the figures below. Stress singularity is a point of the mesh where the maximum stress does not converge to a specific value. So, as we kept refining the mesh, the maximum von-Mises stress values kept increasing. In theory, the stress at the singularity is infinite. As shown in Figure 42, the data diverges.



Figures 40-41: Stress singularities on the model seen after applying a refined mesh.

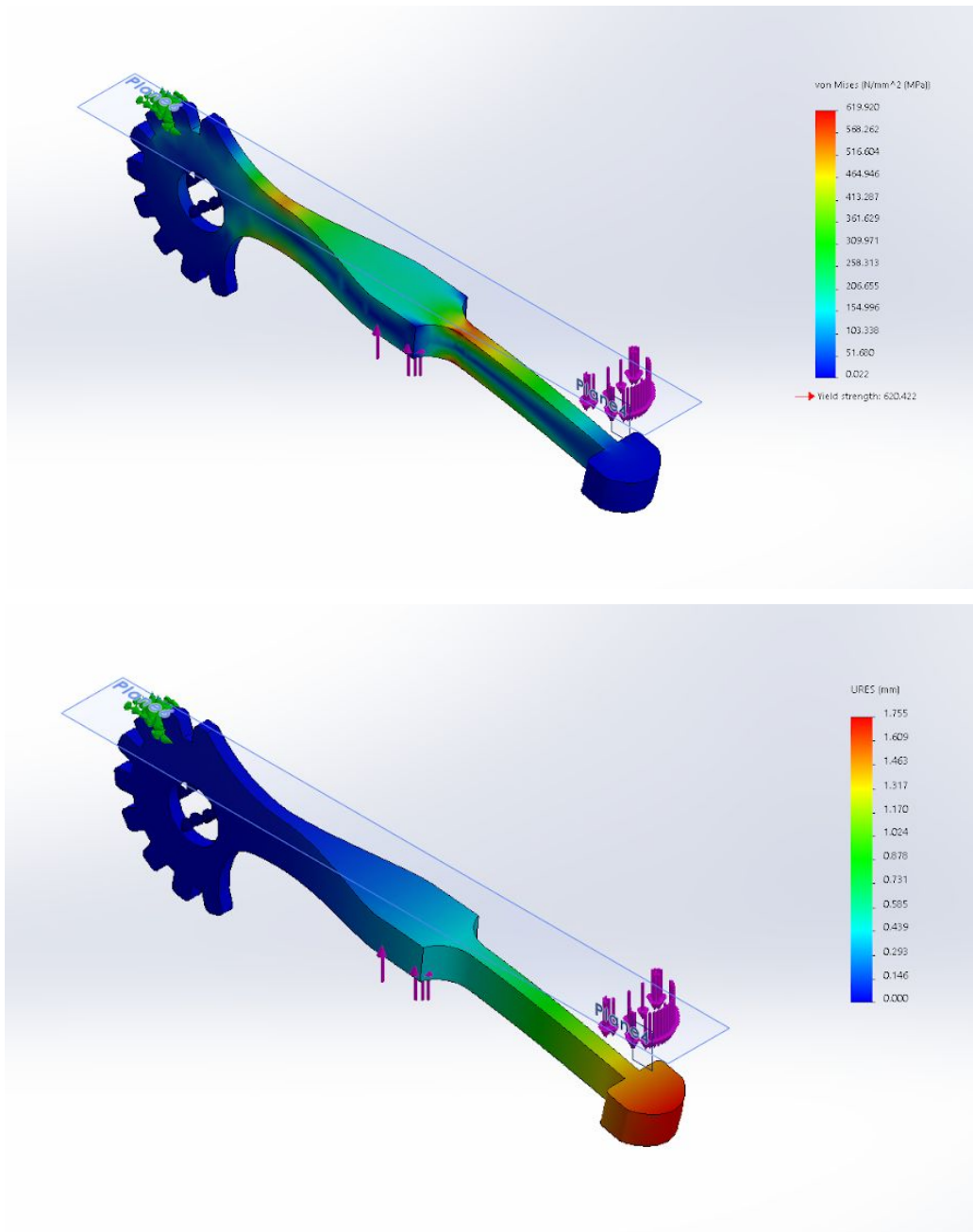
Figure 42



Study 1: Initial Convergence Test (no fillets)							
Global Element Size (mm)	Local Element Size (mm)	Max. Von Mises Stress (MPa)	Max. Axial Displacement (mm)	Number of Nodes (k)	Number of Elements (k)	#DOF (k)	Run Time (hr:min:s)
5	1	822.606	1.86	6.635	3.629	20.010	00:00:01
5	.8	948.715	1.86	7.776	4.278	23.433	00:00:01
5	.5	1071.57	1.87	15.064	8.749	45.297	00:00:02
5	.3	1278.14	1.87	27.815	16.469	83.550	00:00:02
5	.2	1416.62	1.87	40.495	23.697	121.590	00:00:03

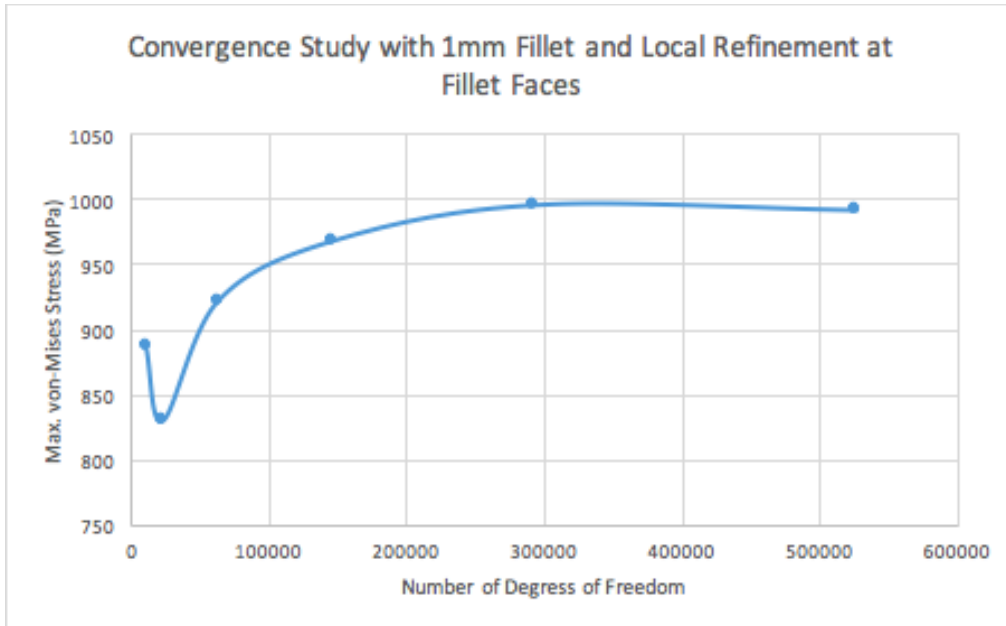
Validation of FEM results

Since there were stress singularities on the initial resulting model, we decided to apply a 1 millimeter fillet radius size on the two sharp edges at the change in geometry to achieve convergence, as shown in Figure 45. Without doing this, our data will never converge to a maximum von-Mises stress value. Also, we want to check if our FEM simulations match our experimental result by looking at what happens in our model in both experimental and FEM results. In our experimental, we saw that the thinner part of the lever had deformed and we wanted to see whether or not the maximum von-Mises stress value would converge so that it would pass the yield strength of the material. This would imply that the model in SolidWorks undergoes plastic deformation. Figure 45 and Study 2 show that the data converges to 995 MPa, which surpasses the yield strength of our material which was 965 MPa. Knowing this, and by the application of the von-Mises failure theory, it can be concluded that our model in SolidWorks had experienced yielding which lead to plastic deformation.



Figures 43-44: Stress and displacement plot results of the implemented fillet radius.

Figure 45



Study 2: Convergence Test with Fillet Radius of 1mm							
Global Element Size (mm)	Local Element Size (mm)	Max. Von Mises Stress (MPa)	Max. Axial Displacement (mm)	Number of Nodes (k)	Number of Elements (k)	#DOF (k)	Run Time (hr:min:s)
5	2	887.823	1.852	3.533	1.745	10.704	00:00:02
5	1	830.385	1.854	7.633	4.219	23.004	00:00:04
5	0.50	922.411	1.856	21.065	12.451	63.300	00:00:05
5	0.30	968.17	1.857	48.683	29.517	146.154	00:00:11
5	0.20	995.639	1.856	97.412	59.974	292.341	00:00:28

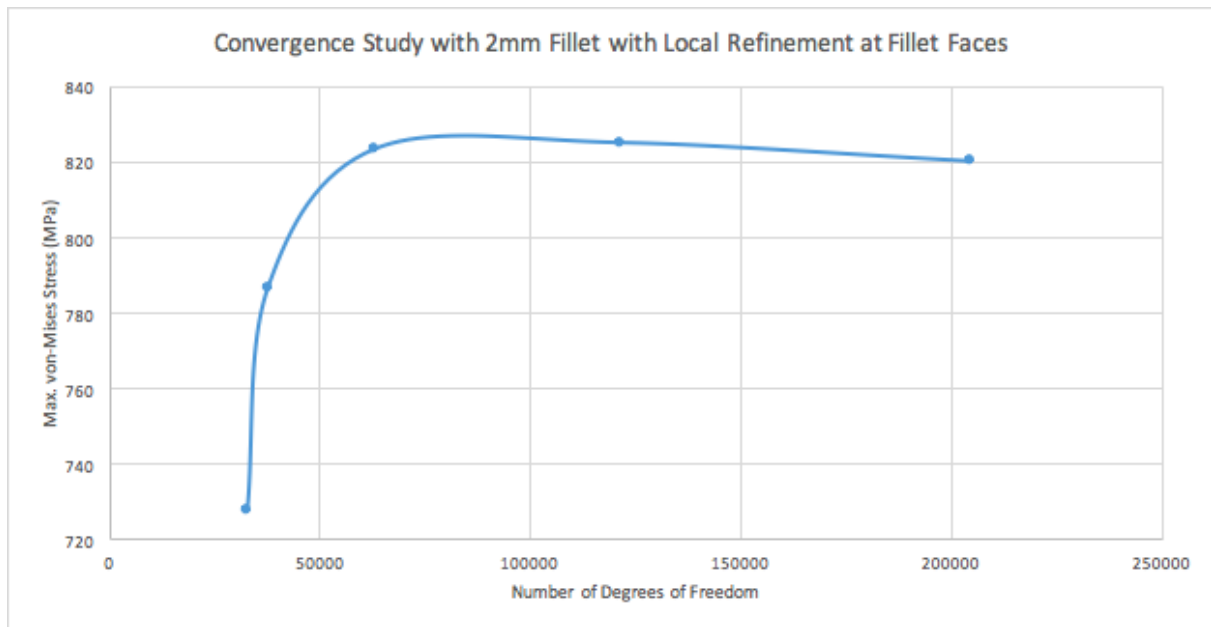
$$\text{Percent Error} = \frac{\text{analytical} - \text{fem results}}{\text{analytical}} * 100 = \frac{1415.13 \text{ MPa} - 995.639 \text{ MPa}}{1415.13 \text{ MPa}} * 100\% = 29.64\%$$

The maximum stress in the analytical results is 1415.13 MPa and is numerical is 995.63 MPa. It has a percent error of 29.64%.

Sensitivity Study

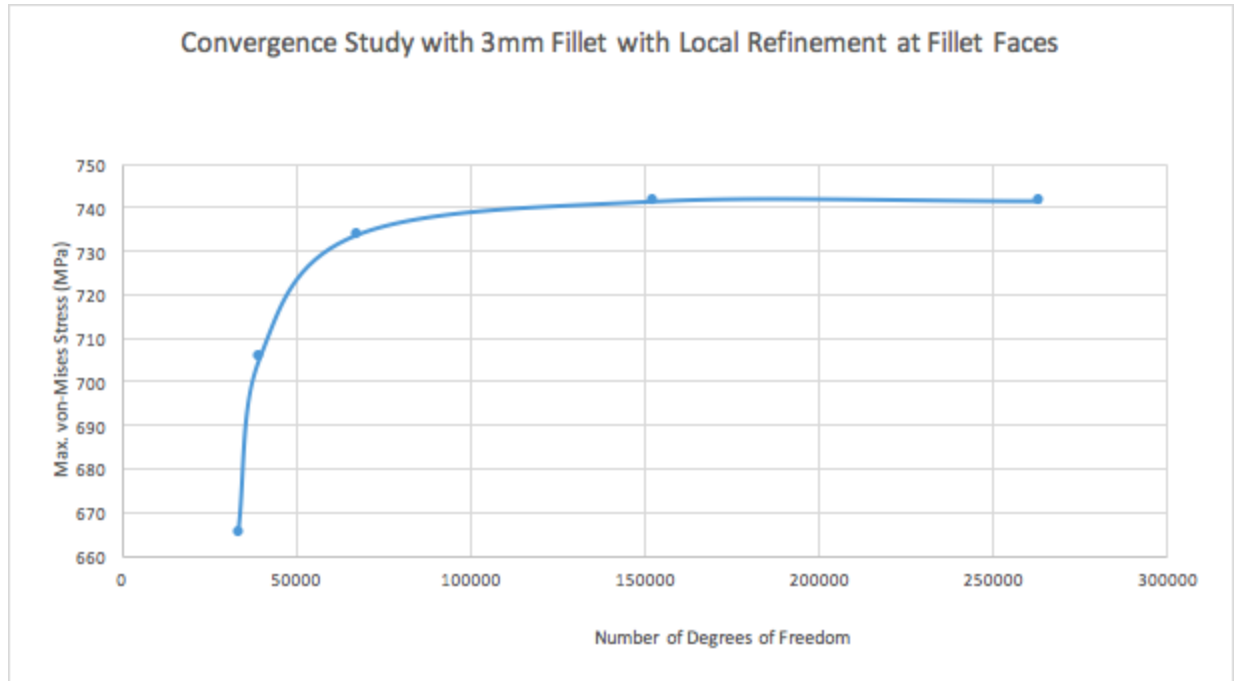
Now that we know the model experienced plastic deformation, we want to perform a sensitivity study to enhance the design of the lever, in which the maximum von-Mises stress should be lower than the yield strength of the material. Our plan was to vary the sizes of the fillets on the two sharp edge corners of the lever and to see the resulting effect in our model. Studies 2-7 and Figures 46-51, show that the maximum von-Mises stress values that converge are less than the yield strength.

Figure 46



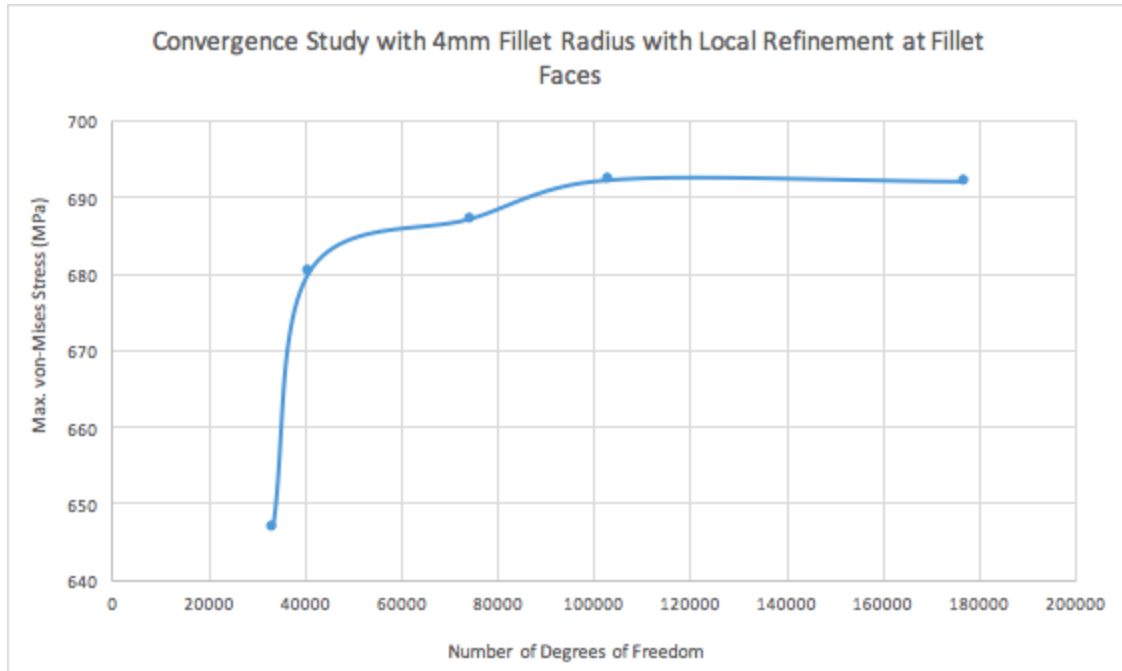
Study 3: Convergence Test with Fillet Radius of 2mm							
Global Element Size (mm)	Local Element Size (mm)	Max. Von Mises Stress (MPa)	Max. Axial Displacement (mm)	Number of Nodes (k)	Number of Elements (k)	#DOF (k)	Run Time (hr:min:s)
5	2	727.6	1.846	10.960	6.084	32.814	00:00:01
5	1	786.9	1.848	12.606	7.116	37.749	00:00:02
5	0.50	823.5	1.847	21.030	12.778	63.021	00:00:05
5	0.30	825.2	1.847	40.451	26.133	121.284	00:00:10
5	0.20	820.3	1.847	68.130	45.410	204.321	00:00:18

Figure 47



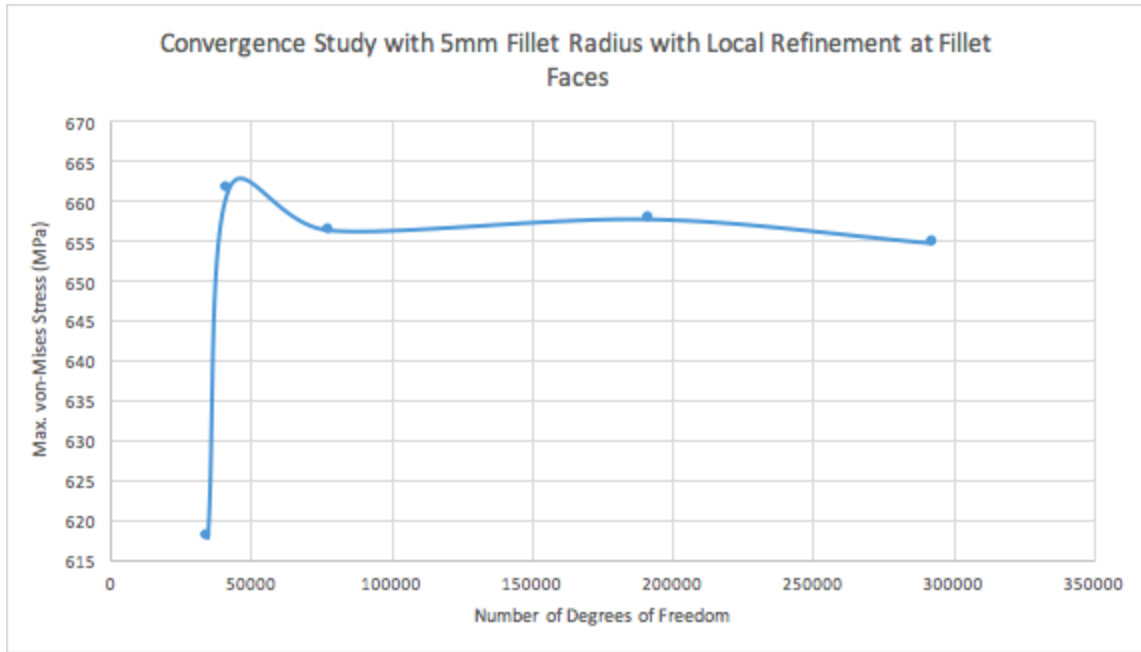
Study 4: Convergence Test with Fillet Radius of 3mm							
Global Element Size (mm)	Local Element Size (mm)	Max. Von Mises Stress (MPa)	Max. Axial Displacement (mm)	Number of Nodes (k)	Number of Elements (k)	#DOF (k)	Run Time (hr:min:s)
5	2	665.2	1.823	11.071	6.190	33.144	00:00:01
5	1	705.5	1.825	13.159	7.498	39.408	00:00:02
5	0.50	733.7	1.825	22.410	13.671	67.161	00:00:05
5	0.30	741.4	1.825	50.680	33.123	151.971	00:00:07
5	0.20	741.5	1.825	87.771	58.864	263.247	00:00:10

Figure 48



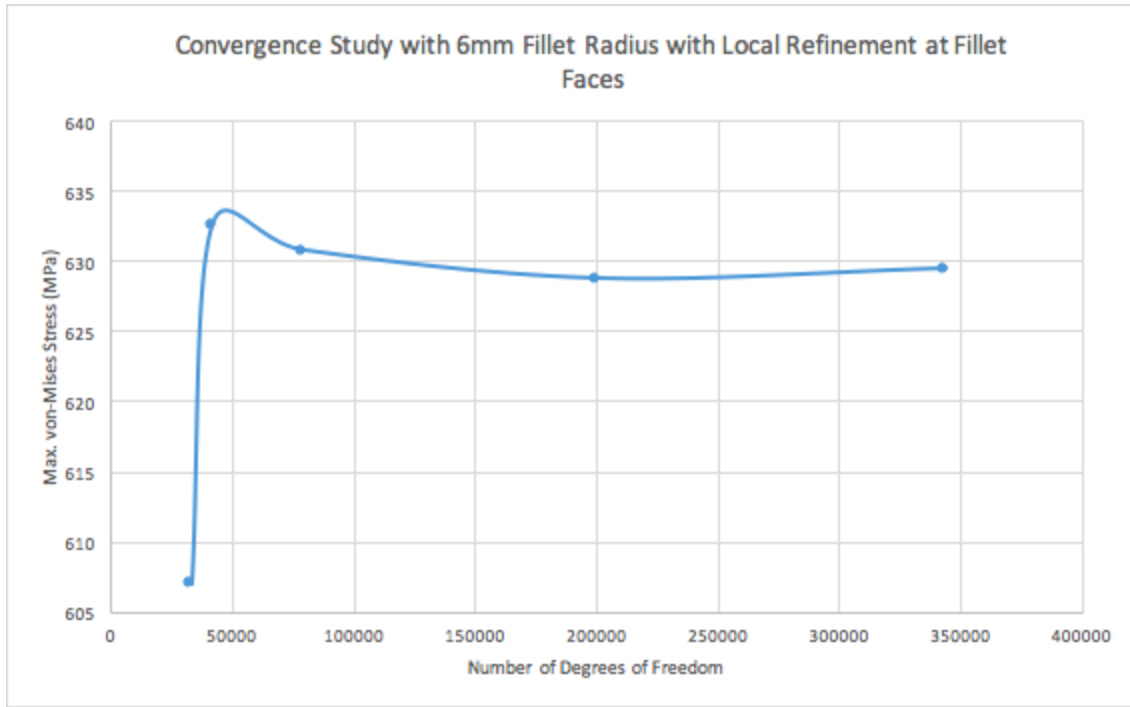
Study 5: Convergence Test with Fillet Radius of 4mm							
Global Element Size (mm)	Local Element Size (mm)	Max. Von Mises Stress (MPa)	Max. Axial Displacement (mm)	Number of Nodes (k)	Number of Elements (k)	#DOF (k)	Run Time (hr:min:s)
5	2	646.9	1.801	11.145	6.199	33.366	00:00:01
5	1	680.5	1.803	13.730	7.837	41.121	00:00:01
5	0.50	687.3	1.801	24.922	15.342	74.697	00:00:05
5	0.30	692.3	1.803	34.459	22.201	103.311	00:00:07
5	0.20	692.1	1.803	59.034	38.716	177.033	00:00:10

Figure 49



Study 6: Convergence Test with Fillet Radius of 5mm							
Global Element Size (mm)	Local Element Size (mm)	Max. Von Mises Stress (MPa)	Max. Axial Displacement (mm)	Number of Nodes (k)	Number of Elements (k)	#DOF (k)	Run Time (hr:min:s)
5	2	617.8	1.779	11.428	6.421	34.215	00:00:01
5	1	661.5	1.781	13.886	7.913	41.589	00:00:01
5	0.50	656.4	1.781	25.977	16.022	77.862	00:00:05
5	0.30	657.8	1.782	63.810	41.958	191.361	00:00:07
5	0.20	654.8	1.781	97.417	65.177	292.182	00:00:10

Figure 50



Study 7: Convergence Test with Fillet Radius of 6mm							
Global Element Size (mm)	Local Element Size (mm)	Max. Von Mises Stress (MPa)	Max. Axial Displacement (mm)	Number of Nodes (k)	Number of Elements (k)	#DOF (k)	Run Time (hr:min:s)
5	2	607.1	1.762	11.036	6.147	33.039	00:00:01
5	1	632.6	1.764	13.854	7.881	41.493	00:00:01
5	0.50	630.8	1.764	26.314	16.226	78.873	00:00:05
5	0.30	628.8	1.764	66.819	44.073	200.388	00:00:07
5	0.20	629.5	1.764	114.645	77.215	343.866	00:00:10

Figure 51

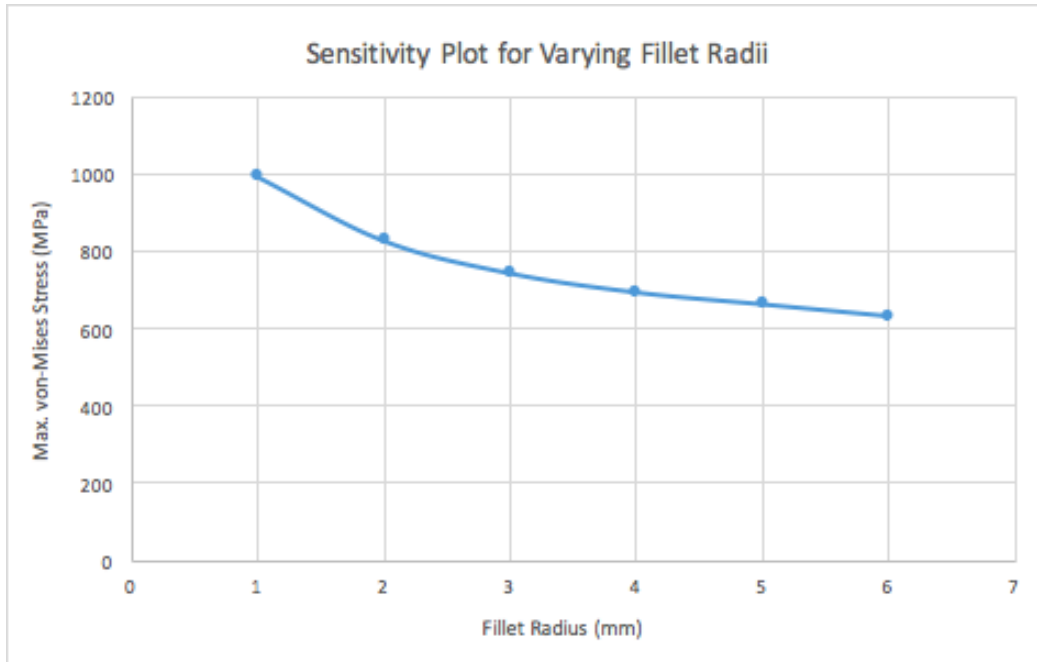


Figure 51 shows that as you increase the fillet size on the sharp edge corners, the maximum von-Mises stress decreases. As you increase the size of the fillet on the sharp edge, the change in geometry is not that drastic anymore. As a result of this, the load paths are able to flow with less restriction.

Implications for Design

From the FEA results that were obtained, one problem area that was found included high stress concentrations around the sharp corners of the lever where a change in geometry was observed. As concluded from our sensitivity study, an addition of a fillet, and later an increase in the fillet radius in this area, would result in a decrease in the maximum von-Mises stress. This means that the stress concentration would not be as high as it originally was at the sharp corner. This change in design would also change the design of the grips of course, as the grips depend on the shape of the cut-out of the levers. The reason why the lever was thinner at the farther end was because the manufacturer left room for the grips to be mounted on top of it. Since the grips were of plastic material, we disregarded them for our model. With a change in the design of the lever from having sharp corners to fillets, the manufacturer would also need to change the design of the grip which can be conflicting in the process of manufacturing this product.

Another way in which this problem area can be fixed is to thicken the thinner part of the lever, thus constricting the thickness of the plastic grips that mount on top of the levers. Thickening the part of the lever that is thin would most likely result in more distributed stresses along the length of the lever. Due to a lack of time on our part, further tests could not be implemented to test this theory. However, a sensitivity test with varying thicknesses of the thinner part of the lever would have to be performed in order to come to a proper conclusion.

Conclusion

Our predictions were close, if not the same, to the results found in the FEM studies. After applying the forces and restrictions from the original free body diagram from Figure 6 into SolidWorks, the maximum von-Mises stress was found at the location of change in geometry as predicted, and the maximum and minimum displacements were found at the far end and sector gear tooth respectively. Prior knowledge from our FEM 2 assignment allowed us to make the prediction that a high stress concentration would be present around the sharp corners at the change in geometry for the part. This meant that the maximum stress would always diverge on the model around that area, which was the case as seen in Study 1. In order to obtain convergence on our model, fillets were applied at the two sharp corners as seen in Figure 43. A sensitivity test using a variety of different fillet sizes showed that as the fillet sizes increased, the maximum von-Mises stress decreased. This is what we had wanted in order to improve the design of the model, as a lesser maximum von-Mises stress means that it is that much smaller than the yield strength. As mentioned before by the use of the von-Mises failure theory, once the maximum stress surpasses the yield, the material goes into yielding which results in plastic deformation. In order to keep the material elastic, it is important to make sure that the maximum von-Mises stress stays within the elastic range of the stress-strain curve of the ductile material, where the elastic range always has a lesser stress than the yield strength. With a change in the design in adding fillets to the sharp corners, the manufacturing process for the product, in particular the grips, could become conflicting. Apart from applying fillets, another change to improve the design might be to vary the thicknesses of the thinner part of the lever. A sensitivity test with this one variable can show whether or not it improves the design of the lever.

There are a lot of inconsistencies throughout our report. The yield strength is too high for a common household item, and the maximum von-Mises forces found in our studies are not all too reasonable. Suggestions given by Professor Benenson such as modifying the boundary conditions, using a lesser applied load, and using a material whose yield strength would be lesser than the one used here, may have provided more reasonable results for our study. Modifying the boundary conditions would have most likely given different problem areas on the model than the one used in this project. To test these suggestions, we ran a simulation using a different boundary condition of only a distributed load on the main part of the lever where the hand would be placed. The fixed geometry and bearing stayed the same and the applied force was set to be 68N. This number was found by doing a test at home with a bathroom scale where the person applied as much force on it with their hands as possible. The greatest amount of force applied was around 30 pounds which is equivalent to 133N. Since one lever involves one hand, 133N was divided by 2 to get 68N of applied force. The material was selected as 301 steel with a yield strength of 205 MPa. Running this study, the initial test diverged and surpassed the yield strength thus undergoing plastic deformation. An addition of fillets allowed convergence to a maximum von-Mises stress of 179 MPa which seems more reasonable for the study we did. Since the

boundary conditions were changed in this scenario, the areas of maximum von-Mises stress and displacements had also changed. The maximum stress was found near the gear tooth of the sector gear with a refined mesh, and some high stress was found near the thinner geometry of the lever near the gear face. This can suggest that the deformities initially found from our experiment, as seen in Figure 4, could have been a result of high stress in the fixed tooth of the gear.

There were many things in this project that could have been done differently, however our approach was in the right direction. We successfully modeled our part in SolidWorks with satisfactory conditions that allowed us to get the same results as those found in our experimental. The material selection process proved to be a problem as every test performed in this project relied heavily on the properties of the chosen material. The conducted hardness and density tests did not provide much information that could've been used to select an appropriate material for our part. One main problem within our group was time management, as we had started the project much later than other groups did. We were limited in time and unfortunately could not carry out all the studies and re-tests that we had wanted to perform within this timeframe. What we learned most from this project was that SolidWorks does not always provide the correct results for a given situation. Our data initially looked right when we were conducting the tests, however it wasn't until Professor Benenson pointed out the flaws that we realized the results were not all too reasonable. Had we started sooner or had been given more time, additional simulations would have been run in order to get the most reasonable results for the failure analysis that we chose to perform on the corkscrew.

References

- [1] <http://www.carbidedepot.com/formulas-hardness.htm>
- [2] <https://www.simscale.com/docs/content/simwiki/fea/whatisfea.html>
- [3] <http://matweb.com/search/DataSheet.aspx?MatGUID=7ab1936975fd4cb2937286a8a004e052&ckck=1>